Dynamic structure factor for classical motion in one-dimensional potentials

C. A. Condat
Department of Physics, University of Puerto Rico at Mayagüez, Mayagüez, Puerto Rico 00700

J. Jäckle
Fakultät für Physik, Universität Konstanz, D-7750 Konstanz, Germany
(Received 21 October 1991)

The dynamical correlation functions are considered for classical particles moving in general one-dimensional unbounded potentials. In particular, the dynamic structure factor $S(k,\omega)$, which predicts the intensity measured in a neutron-scattering experiment, is calculated in detail. According to the magnitude of the energy transfer, the analysis of $S(k,\omega)$ is usually divided into three regions: inelastic, quasielastic, and elastic. New results are obtained for each region: (a) The presence of a band structure in the inelastic zone, which often exhibits a rich intraband oscillatory behavior. The origin of these oscillations is discussed in detail. (b) The impossibility of having a quasielastic peak if the motion of the scatterer is Hamiltonian, with the important exception of particles moving in potentials that contain horizontal segments. (c) From a comparison between the elastic intensity and the Debye-Waller factor, which gives the elastically scattered intensity when weak frictional forces are added, it is argued that the difference between both functions gives the total quasielastic intensity in the presence of weak friction. The effect of a directional average and of the average over a parameter distribution are also investigated. The general results are illustrated with representative examples.

I. INTRODUCTION

The two-level model has been successfully used to explain the results of thermal and acoustic experiments in low-temperature ($t \leq 1$ K) glasses.[1-3] The two levels considered are the two lowest quantum states for a particle moving in a double-well potential. The height of the central barrier is estimated to lie in the range 100–1000 K.[4] The double-well concept has also been used to explain various relaxation effects at intermediate temperatures.[5-9] Another possible field of application is that of protein dynamics, where a number of interesting neutron-scattering experiments have been recently reported.[10-13] The existence of two-level systems analogous to those in glasses has also been proposed for proteins.[14] At temperatures of the order of 100 K and higher, the motion of the particle can be considered to be approximately classical. Therefore, it is of interest to predict the contribution of the anharmonic states to the dynamical correlation functions in the classical regime. In this paper we study this problem by presenting and exemplifying some general results for the dynamical structure factor (DSF) originated in anharmonic and multiple-well potentials. Some of our conclusions for the inelastic region of the spectrum were included in Ref. 15.

Double-well potentials are also used to define the local modes that characterize the phase transitions in ferroelectrics.[16,17] This motivated an important work by Onodera, who calculated exactly the dynamical susceptibility $S(\omega)$ for a classical anharmonic oscillator.[18] He considered oscillators moving in the potential $V(x)=Ax^4+Bx^2$, with $A>0$ and B either positive or negative. Later, Matsubara noted that $S(\omega)$ for a general one-dimensional potential could be calculated with relative ease due to the periodicity of the solution $x(t)$ of the equation of the motion.[19] This periodicity permits an expansion of $x(t)$ in a Fourier series, which leads to a considerable simplification and a better understanding of the problem. Iwamatsu and Onodera took advantage of this procedure to compute the dynamical structure factor $S(k,\omega)$ for Onodera's anharmonic potential.[20]

After Vineyard calculated $S(k,\omega)$ for the harmonic oscillator,[21] this function has been worked out for many different problems. We should mention here the case of the two-level potentials,[22] which has been used to interpret, for instance, the observations of hydrogen tunneling in niobium compounds.[23] The dynamic structure factors for various types of diffusive and random-walk motion have been computed and applied.[24-28] Schilling and Aubry obtained the static structure factor for an incommensurate structure, which, at low temperatures, gives essentially the magnitude of the elastic part of the DSF.[29] The DSF for a Brownian particle in a cosine potential was calculated by Dieterich, Geisel, and Peschel by solving the corresponding Fokker-Planck equation.[30] There is also a large body of literature on the $S(k,\omega)$ for liquids[31] and on approximate methods like the impulse approximation.[32] Benoit showed that a moments method can be used to evaluate accurately the coherent scattering cross section for general harmonic solids.[33] However, the paucity of exact results for $S(k,\omega)$ in relatively complicated potentials is remarkable. In this area Ref. 20 stands alone.

It is therefore of interest to discuss general properties of the dynamical correlation functions in multiple-well potentials. In Sec. II, we apply the procedure suggested by Matsubara[19] to obtain general results for the dynamical correlation functions in unbounded, one-dimensional

potentials. In the remainder of the paper we study the DSF in detail. It is convenient to divide its analysis according to the magnitude of the energy transferred in the scattering process. Thus, we consider separately the elastic line ($\omega=0$), the quasielastic region (the neighborhood of $\omega=0$), and the inelastic region (away from $\omega=0$).

In Sec. III, we analyze the inelastic region. We find that the scattering potentials can be classified into three well-defined categories, depending on their asymptotic behavior. For two of these categories a rich peak structure appears at high enough values of the temperature and the momentum transfer. We discuss the origin and nature of these peaks and present explicit results for two examples. These examples, the double-parabola and linear single-well potentials, exhibit typical features of two of the potential classes. A case in the third category, in which such peaks do not occur, was discussed 15 years ago in Ref. 20.

We treat the quasielastic (QE) region in Sec. IV. We show that no QE peak can be generated by a one-dimensional Hamiltonian system unless the potential contains a genuinely flat region.

We consider the elastic line $S_{\rm el}(k,T)$ as well as the Debye-Waller factor $f(k,T)$ in Sec. V. The meaning of both functions is discussed and clarified. The Debye-Waller factor correctly predicts the "temperature effect" on the elastic scattering only for low values of the momentum transfer. However, it does give the correct surviving elastic intensity for all k when a small amount of friction is added. We argue that the difference between the total elastic intensity for the Hamiltonian problem [obtained from $S_{\rm el}(k,T)$] and the Debye-Waller factor gives the total QE intensity in the case of low friction.

In practice, we seldom have a sample containing a set of identical wells with a unique spatial orientation. Thus, an experimental result represents, in general, an average over different well shapes and orientations. We discuss two types of averages in Sec. VI: first, the directional average, which takes into account the randomness in the orientation of the scattering centers in a three-dimensional sample; second; the configurational average, which must be performed when there is a distribution of potential parameters in the sample. This work ends with a short discussion in Sec. VII.

II. FORMULATION OF THE PROBLEM

A. Some considerations on periodic motion

We consider dynamic correlation functions for particles moving in a one-dimensional potential $V(x)$. This potential may have one or more minima and satisfies the condition $V(|x|\to\infty)\to\infty$. A particle having energy E performs a periodic motion whose period depends on the explicit form of the potential. The constant energy lines defined by the maxima of $V(x)$ divide the classically allowed region of the x-E plane into domains corresponding to different types of periodic solution. The x-p phase plane is equally divided into different regions for the different domains. It may be convenient to introduce further divisions if the functional form of $V(x)$ changes at sites other than the extrema. For the unbounded double-well potentials shown in Fig. 1, three such domains need to be distinguished: two for oscillations in either well at energies below the maximum barrier energy Q, and a third one for oscillations across both wells at energies E above Q. The period in the jth domain is given by a single-valued function $T_j(E)$. It can be calculated as an integral between the turning points $x_{j1}(E)$ and $x_{j2}(E)$,

$$T_j(E)=(2m)^{1/2}\int_{x_{j1}(E)}^{x_{j2}(E)}[E-V(x)]^{-1/2}dx\ , \tag{2.1}$$

where m is the mass of the particle. The corresponding frequency is $W_j(E)=2\pi[T_j(E)]^{-1}$.

The qualitative behavior of the functions $W_j(E)$ is determined by the types of maxima and minima of $V(x)$, and by the asymptotic form of this function for large x. Three general results for $W_j(E)$ follow directly from Eq. (2.1).

(1) Consider the uppermost energy domain, labeled by $j=J$ and extending from $E=Q_{\rm max}$ up to $E=\infty$. If $V(x)\sim A|x|^q$ when $|x|\to\infty$, then

$$W_J(E\gg Q_{\rm max})\sim E^{1/2-1/q}\ . \tag{2.2}$$

This result means that $W_J(E\to\infty)\to 0$ for $q<2$ and that $W_J(E\to\infty)$ diverges for $q>2$. If $q=2$, $W_J(E)$ goes to a finite oscillation frequency as $E\to\infty$.

(2) Suppose now that $V(x)$ has a minimum at x_0. If in the neighborhood of the minimum it has the form

$$V(x)=E_0+A|x-x_0|^q\quad (q>0)\ , \tag{2.3}$$

we obtain

$$W(E)\sim(E-E_0)^{1/2-1/q}\ . \tag{2.4}$$

For a quadratic minimum (i.e., for $q=2$), $W(E)$ for $E\to E_0$ goes to the finite frequency of small-amplitude oscillations around the potential minimum. If $q\neq 2$, $W(E_0)$ is either zero ($q>2$) or infinite ($q<2$).

(3) If $V(x)$ has a quadratic maximum of height Q—as is the case with the quartic potential treated by Onodera[18] and Iwamatsu and Onodera,[20] $W(E)$ goes logarithmically to zero according to

$$W(E)\sim a_{\gtrless}/\ln\left[\frac{b}{|E-Q|}\right]\ , \tag{2.5}$$

with positive constants $a_>, a_<=2a_>$ and b, for E approaching Q from above ($>$) or below ($<$). If near the maximum $V(x)$ has the form $V(x)=Q-A|x-x_0|^q$ and $q>2$, then $W(E)$ follows a power law in $|E-Q|$ with the same exponent as in (2.4). If $q<2$, there is a discontinuous decrease in $W(E)$ as the energy exceeds the barrier energy Q.

In Fig. 1 we sketch the functions $W(E)$ for three special double-well potentials each of which corresponds to one of the three possibilities for asymptotic behavior, as described under (1). For the double parabola [Fig. 1(a)], $W(E\to\infty)$ is equal to the harmonic-oscillator frequency ω_0. The cusplike maximum leads to a discontinuous period doubling at the threshold energy Q. For the piecewise linear double-well potential [Fig. 1(b)], $W(E)$ is also

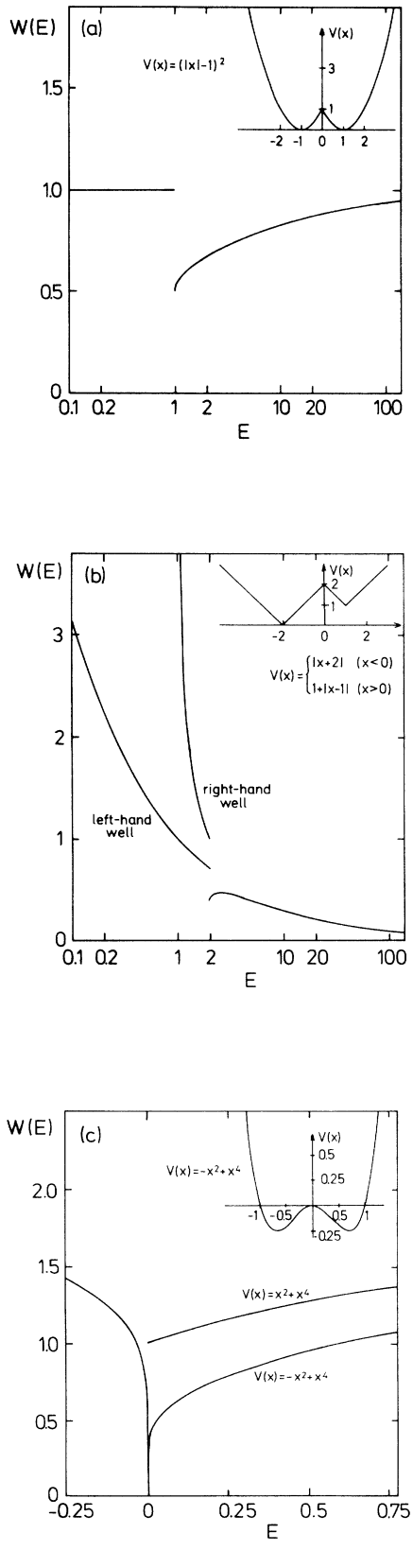

FIG. 1. Fundamental frequency $W(E)$ for three simple potentials (sketched in the insets): (a) double-parabola potential, (b) asymmetric, piecewise linear double-well potential, and (c) quartic potential.

discontinuous at the threshold energy. It goes to zero for $E \to \infty$ and diverges for $E \to 0$. Since the potential drawn is asymmetric, for energies $E < Q$ below the threshold two different branches of the function $W(E)$ exist, one corresponding to each domain. For the potential [Fig. 1(c)], which was treated in Refs. 18 and 20, $W(E)$ goes to zero near the threshold energy [Eq. (2.5)] and diverges for $E \to \infty$.

B. The classical formula for the correlation function

Let $f[x(t)]$ be a dynamical variable which is a function of time through its dependence on the time-dependent position coordinate $x(t)$. We are interested in the classical correlation function

$$\langle f[x(t)]f[x(0)]\rangle = Z^{-1}\int\int_{-\infty}^{+\infty} dx\,dp\, e^{-\beta H(x,p)} f[x_t(x,p)]f(x) , \tag{2.6}$$

where $H(x,p)$ is the Hamiltonian and $x_t(x,p)$ is the position coordinate at time t, expressed as a function of the position coordinate x and momentum p at time zero. $\beta=(k_B T)^{-1}$, where T is the temperature and k_B is Boltzmann's constant. Z is the classical partition function given by

$$Z=\int\int_{-\infty}^{+\infty} dx\,dp\, e^{-\beta H(x,p)} = \sum_j \int_{E_{jl}}^{E_{ju}} dE\, e^{-\beta E} T_j(E) . \tag{2.7}$$

Here E_{jl} and E_{ju} denote the lower and upper limit of the energy in the jth domain. Following Matsubara,[19] for each domain the integral in the phase plane can be transformed into an integral over energy and time, where the time integration extends from zero to the period $T_j(E)$. The Jacobian of this transformation can be shown to be unity. Putting

$$x = x_j(E,t_0)$$

and

$$x_t(x,p) = x_j(E,t_0+t) ,$$

where $x_j(E,t)$ is the solution of Newton's equation for the position coordinate at energy E in domain j, we can write the correlation function (2.6) as

$$Z^{-1}\sum_j \int_{E_{jl}}^{E_{ju}} dE\, e^{-\beta E} \times \int_0^{T_j(E)} dt_0 f[x_j(E,t_0+t)]f[x_j(E,t_0)] . \tag{2.8}$$

Expanding the periodic function $f[x_j(E,t)]$ in a Fourier series

$$f[x_j(E,t)] = \sum_{n=-\infty}^{+\infty} F_{jn}(E) e^{inW_j(E)t} , \tag{2.9}$$

with Fourier coefficients

$$F_{jn}=[T_j(E)]^{-1}\int_0^{T_j(E)} dt\, e^{-inW_j(E)t} f[x_j(E,t)] , \quad (2.10)$$

we obtain the following result for the Fourier transform of the correlation function:[19,20]

$$S_{f,f}(\omega)=(2\pi)^{-1}\int_{-\infty}^{\infty} dt\, e^{i\omega t}\langle f[x(t)]f[x(0)]\rangle$$
$$=Z^{-1}\sum_j \sum_{n=-\infty}^{+\infty} \int_{E_{jl}}^{E_{ju}} dE\, e^{-\beta E} T_j(E)|F_{jn}(E)|^2$$
$$\times\delta[\omega-nW_j(E)] . \quad (2.11)$$

This formula is the starting point of our calculations of the dynamic structure factor $S(k,\omega)$, which is obtained for $f(x)=e^{ikx}$. The wave-vector dependence of $S(k,\omega)$ arises from the additional k dependence of the Fourier coefficients (2.10), which we denote by $F_{jn}(E,k)$.

It is worthwhile to compare the classical result (2.11) with the quantum-mechanical formula, in which $S(k,\omega)$ is expressed as a sum over initial and final quantum-mechanical states. The factor $T_j(E)$, together with the sum over the different domains j, corresponds to the quantum-mechanical level density, which in the semiclassical Bohr-Sommerfeld approximation is given by the period $T(E)$ divided by Planck's constant h. The Fourier coefficients $F_{jn}(E,k)$ replace the quantum-mechanical matrix elements, and the energy transfer $\hbar\omega$, which in the quantum-mechanical case is given by the energy difference between the final and initial state, is equal to multiples of the oscillation frequency $W(E)$ times $\hbar$.

III. INELASTIC SCATTERING: OSCILLATIONS

A. Origin of the oscillations

The Fourier coefficients $F_{jn}(E,k)$ are oscillatory functions of both k and E. For the simple harmonic oscillator, e.g., they are given by

$$F_n(E,k)|_{\rm HO}=J_n[kA(E)] ,$$

where $A(E)=(2E/m\omega_0^2)^{1/2}$ is the amplitude of the oscillation at energy E. The Bessel functions J_n are oscillatory functions of the argument.

For every integer n and domain j, the δ function $\delta[\omega-nW_j(E)]$ defines a mapping of the energy interval $E_{jl}\le E\le E_{ju}$ of that domain on a certain range of ω. The properties of this mapping depend on the functional form of the fundamental frequency $W_j(E)$. It may compress or dilate the oscillatory features exhibited by the Fourier coefficients $F_{jn}(E,k)$ as a function of E. In the energy regions where $W_j(E)$ varies very slowly, a wide E interval contributes to a narrow ω interval. The oscillations that appear in $F_{jn}(E,k)$ will be then projected onto a small frequency range, giving rise to a rich peak structure in $S(k,\omega)$, provided that temperature and wave vector are large enough.

Considering potentials that grow as $|x|^q$ when $|x|\to\infty$, we see from Eq. (2.2) that $\delta[\omega-nW_j(E)]$ projects an infinite portion of the uppermost energy domain onto a finite ω range if $q\le 2$. When $q<2$, the point $\omega=0$ will be an accumulation point for the projected oscillations of $F_{jn}(E,k)$. In the case $q=2$, the natural oscillator frequency will serve as the corresponding accumulation point. If $q>2$, the uppermost energy domain is mapped onto an infinite range and there is no accumulation point, the oscillations of $F_{jn}(E)$ not being strongly compressed by the mapping. This is the reason why no rapid oscillations occur in Ref. 20.

When considering more general unbounded potentials, it is convenient to divide them into three classes: (a) $V(x)\sim Cx^2$ for large x, (b) $V(x)<Cx^2$ for all x larger than a certain constant M, and (c) $V(x)>Cx^2$ for all x larger than M. One example in each class is presented in Fig. 1. From the preceding discussion it follows that $\omega=0$ will be an accumulation point for the oscillations in $S(k,\omega)$ for all potentials in class (b). There will be no such accumulation point for potentials in class (c).

We can also see from Eq. (2.11) that more than one energy may contribute to $S(k,\omega)$ for each ω. This is exemplified by the three cases depicted in Fig. 1. The relative importance of the various contributions will depend on the temperature through the Boltzmann factor.

Next we analyze in detail the inelastic spectrum for one example in each of the classes (a) and (b). An example for potentials in class (c), the quartic potential, was studied in Ref. 20.

B. The double-parabola potential

We consider the double-parabola (DP) potential with minima at $\pm l$,

$$V(x)=\tfrac{1}{2}m\omega_0^2(|x|-l)^2 . \quad (3.1)$$

[See Fig. 1(a).] This is a potential in class (a), with a central barrier whose height is $Q=m\omega_0^2 l^2/2$. The barrier and the line $E=Q$ define three domains. The motion in each of the two $E<Q$ domains, which are identical, is purely harmonic with a frequency $W(E)=\omega_0$. If $E>Q$, the frequency is given by

$$W(E)=\omega_0[1+(2/\pi)\arcsin(Q/E)^{1/2}]^{-1} . \quad (3.2)$$

The function $W(E)$ jumps from ω_0 to $\omega_0/2$ at $E=Q$ and then grows monotonically, approaching $\omega=\omega_0$ as $E\to\infty$.

Using Eqs. (2.7) and (3.2), we can calculate the partition function,

$$Z=\frac{2\pi}{\omega_0\beta}\left[2-e^{-\beta Q}+\frac{2\beta Q}{\pi}\int_1^{\infty} dx\, e^{-\beta Q x}\Psi(x)\right] , \quad (3.3)$$

where we wrote $x=E/Q$ and $\Psi(x)=\arcsin(x^{-1/2})$. The factor inside the large square brackets decreases monotonically from two to one as Q decreases from infinity down to zero. This was to be expected, since at very low temperatures ($\beta Q\gg 1$) we have two simple oscillators, while at high temperatures ($\beta Q\ll 1$) the particle is effectively subject to a single harmonic oscillator.

It is convenient to write the solution to the equation of motion in the $E>Q$ region as

$$x(E,t)=\begin{cases} l+A\sin(\omega_0 t-\Psi), & 0\le t<\frac{1}{2}T(E) , \\ -l+A\sin(\omega_0 t-3\Psi), & \frac{1}{2}T(E)\le t<T(E) , \end{cases} \quad (3.4)$$

where $A=(2E/m\omega_0^2)^{1/2}$ is the harmonic-oscillator amplitude and Ψ is defined above. This equation describes a complete period and is then suitable for the calculation of the Fourier coefficients (2.10). If $E<Q$ the solution is simply

$$x(E,t)=\pm l - A\sin(\omega_0 t)\ . \tag{3.5}$$

We first find the contribution $S^<(k,\omega)$ of the $E<Q$ region. The Fourier coefficients $F_n(E)$ are proportional to the Bessel functions $J_n(kA)$, and we obtain a superposition of δ functions at integer, multiples of ω_0:

$$S^<(k,\omega)=(4\pi/\omega_0 Z)\sum_{n=-\infty}^{\infty}\int_0^Q dE\, e^{-\beta E}|J_n[kA(E)]|^2 \times\delta(\omega-n\omega_0)\ . \tag{3.6}$$

The coefficients $S_n^<$ of the first four δ functions are plotted in Fig. 2 for a representative value of the momentum transfer k. The intensity of the elastic peak decreases monotonically as a function of the temperature, whereas each of the $|n|>0$ peaks has a single maximum at a finite temperature. The position of this maximum shifts slowly towards higher temperatures when $|n|$ is increased. In the low-T limit, and for $n>0$, S_n grows as a power law, $S_n^<\sim(T/Q)^n(kl)^{2n}$. If $Q\to\infty$, Eq. (3.6) leads to the well-known harmonic-oscillator result.[21]

Next we present the results for the contribution $S^>(k,\omega)$ of the $E>Q$ region. The $n=0$ term in the Fourier expansion (2.11) yields an elastic peak, which will be discussed in Sec. V. The other components generate the factorized expression

$$S_{\rm in}^>(k,\omega)=\sum_{n\neq 0} f_n(\omega,T)|g_n(\omega,k)|^2\ , \tag{3.7}$$

where the nth term contributes only in the frequency range $n\omega_0/2\le\omega\le n\omega_0$. We call this contribution the nth band. The temperature appears only in the function

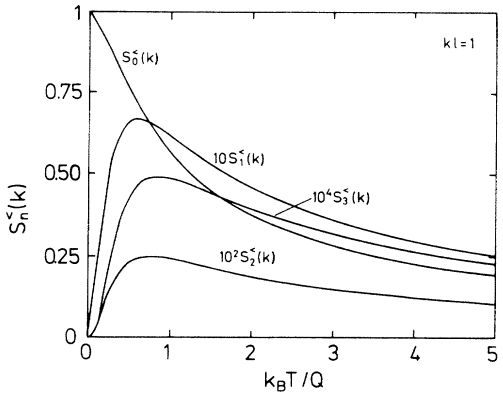

FIG. 2. Dynamical structure factor for the DP potential: The contribution of the $E<Q$ region as a function of temperature for $kl=1$. The curve $S_n^<(k)$ represents the prefactor of $\delta(\omega-n\omega_0)$ in Eq. (3.6). The low-T behavior is given by $S_n^<\sim(T/Q)^n(kl)^{2n}$. Note that each curve is plotted using a different scale.

$f_n(\omega,T)$, which has the form

$$f_n(\omega,T)=\frac{2Q}{\omega_0 Z}\left[\frac{\omega_0}{\omega}\right]^3 n^2\left|\sin\left[\frac{\pi n\omega_0}{2\omega}\right]d^{-3}(\omega)\right| \times\exp[-\beta Q d^{-2}(\omega)]\ , \tag{3.8}$$

where $d(\omega)=\cos(\pi n\omega_0/2\omega)$. The sine generates zeroes at the lower band edges $[\omega\to(n\omega_0/2)^+]$, while the Boltzmann factor generates zeroes at the upper band edges $[\omega\to(n\omega_0)^-]$, where

$$f_n\sim\exp[-4\beta Q(n\omega_0/\pi)^2(\omega-n\omega_0)^{-2}]\ .$$

The factor

$$g_n(\omega,k)=\int_0^\pi dy\cos\left[kl\left\{1+d^{-1}(\omega)\cos\left[\frac{n\omega_0}{\omega}\left[y-\frac{\pi}{2}\right]\right]\right\}-ny\right] \tag{3.9}$$

contains all the k dependence. It has the form of a generalized Bessel function and oscillates rapidly as $\omega\to(n\omega_0)^-$. The upper band edge is indeed an accumulation point for the oscillations. With increasing k the oscillations start at lower frequencies.

We plot f_1 and g_1 as functions of the frequency in Fig. 3. The height of the maximum in f_1 increases with the temperature. Increasing T also shifts the position of the maxima towards higher frequencies. Thus, when we form the product $f_1|g_1|^2$, the oscillations in g_1 are suppressed by the Boltzmann factor at low temperatures, but they become evident when T is high enough. Alternatively, the oscillations can be exhibited by increasing the value of kl, which pulls them towards lower frequencies.[15] These features can be seen in Figs. 4–6. In Fig. 4 we take $kl=1$ and show the effect of increasing T; several maxima appear near the upper-band edges when

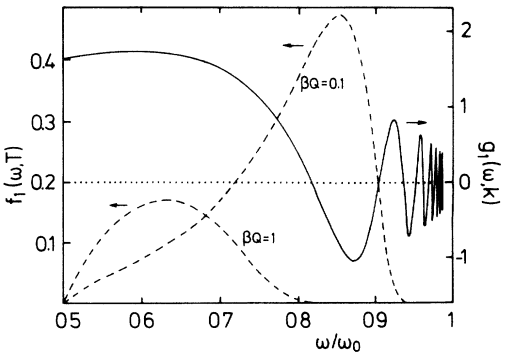

FIG. 3. The two factors that form $S_{\rm in}^>(k,\omega)$ in the fundamental band ($n=1$) for the DP potential. The dashed lines represent f_1 for the indicated temperatures, whereas the solid curve represents the integral g_1 for $kl=1$.

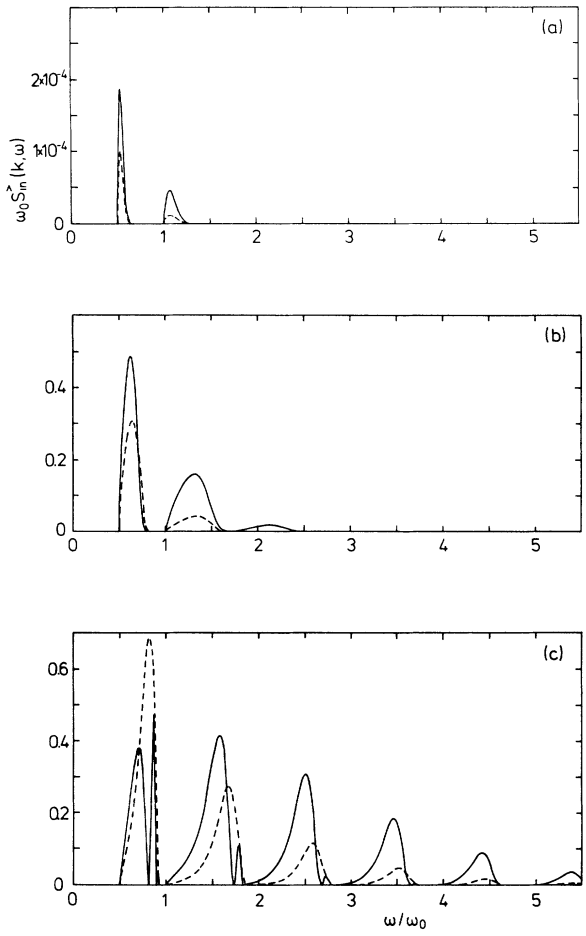

FIG. 4. Effect of varying the temperature on $S_{in}^{>}(k,\omega)$ for the DP potential (solid lines). Here $kl=1$ and the temperatures are (a) $k_BT/Q=0.1$, (b) $k_BT/Q=1$, and (c) $k_BT/Q=10$. The dashed lines represent the directional averages (see Sec. VI).

$k_BT/Q=10$. In Fig. 5, we choose $k_BT/Q=1$ and $kl=10$. Each band exhibits several maxima, and the oscillations are not restricted to the neighborhood of the upper-band edges. Note also the overlapping of the $n>1$ contributions. In Fig. 6, we plot the first band for high values of the temperature ($k_BT/Q=10$) and the momentum transfer ($kl=10$). The combination of both favorable circumstances creates an impressive peak structure.

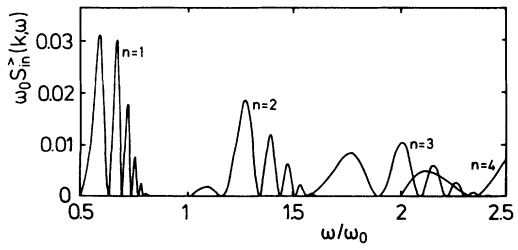

FIG. 5. $S_{in}^{>}(k,\omega)$ for the DP potential at high momentum transfer ($kl=10$). Here $k_BT/Q=1$ and the different terms in Eq. (3.7) have been plotted separately.

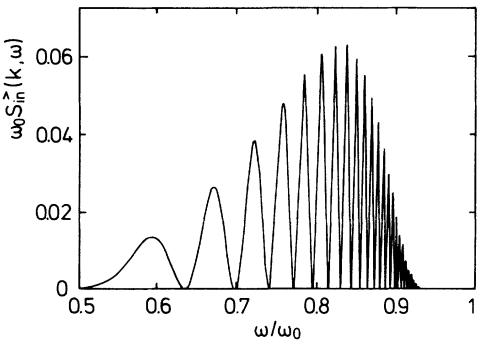

FIG. 6. The fundamental band ($n=1$) of $S_{in}^{>}(k,\omega)$ for the DP potential at high values of the temperature ($k_BT/Q=10$) and momentum transfer ($kl=10$).

A different representation is shown in Fig. 7, where the dynamic structure factor is plotted as a function of the wave number for two frequencies in the first band ($n=1$) and one in the second band ($n=2$).

Some further points should be noted.

(1) None of the potential domains gives any quasielastic contributions. Apart from the elastic line, $S(k,\omega)$ is strictly zero for $|\omega|<\omega_0/2$.

(2) The sum rule $\int S(k,\omega)d\omega=1$ must always be satisfied.[24] For the DP potential, intensity is transferred between the δ functions in $S^{<}$ and the continuum distribution $S_{in}^{>}$ (plus the elastic line $S_0^{>}$) when the temperature is increased. For the quartic potential, on the other hand, the lower potential domains are not harmonic and the intensity transfer takes place between two continuum distributions.

(3) Comparing Figs. 4 and 5 we note that, at a given temperature, the contributions of higher values of ω are stronger (and those of lower ω weaker) for larger values of the momentum transfer. This is consistent with the moment sum rule $\langle\langle\omega^2\rangle\rangle=k^2/(m\beta)$ (see Ref. 24).

C. The linear single-well potential

We now choose a simple example of a potential in class (b),

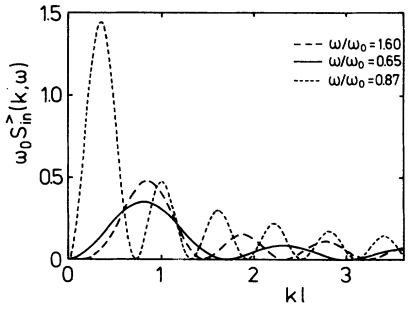

FIG. 7. $S_{in}^{>}(k,\omega)$ as a function of kl for the indicated frequencies. Here $k_BT/Q=10$. The highest value of the frequency lies in the second band ($n=2$).

$$V(x)=\alpha|x| \ . \tag{3.10}$$

There is no internal potential hill setting a natural energy scale, and there is obviously a single domain in the x-E plane. The turning points for a particle moving with energy E in this potential are $\pm X=\pm E/\alpha$. Its period is

$$T(E)=(32mE)^{1/2}/\alpha \ . \tag{3.11}$$

Consequently, the function $W(E)$ takes all positive values. The partition function can be calculated easily. We obtain,

$$Z=(8\pi m/\alpha^2\beta^3)^{1/2} \ . \tag{3.12}$$

The solution to the equation of motion is

$$x(E,t)=\begin{cases} X[1-(1-4t/T)^2], & 0\le t<\frac{1}{2}T \ , \\ X[-1+(1+4t/T)^2], & \frac{1}{2}T\le t<T \ . \end{cases} \tag{3.13}$$

A calculation similar to that performed for the DP potential yields

$$S(k,\omega)=S_{\rm el}(k,\omega)+S_{\rm in}(k,\omega) \ , \tag{3.14}$$

where $S_{\rm el}$ represents the intensity of the elastic line and the inelastic term is given by

$$\tilde{\omega}S_{\rm in}(k,\omega) = \frac{4}{\pi^{1/2}}\left[\frac{\tilde{\omega}}{\omega}\right]^4 \sum_{n=1}^{\infty} n^3\exp[-(n\tilde{\omega}/\omega)^2]|R_n|^2 \ . \tag{3.15}$$

The integrals R_n are defined as

$$R_n=\int_0^1 dx\,\cos[k\tilde{l}n^2(\tilde{\omega}/\omega)^2(x^2-x)+n\pi x] \ , \tag{3.16}$$

and we have introduced the temperature-dependent frequency

$$\tilde{\omega}(T)=(\beta/8m)^{1/2}\pi\alpha \ , \tag{3.17}$$

and length

$$\tilde{l}(T)=4/\alpha\beta \ . \tag{3.18}$$

If desired, the integrals R_n can be expressed in terms of Fresnel functions. The effect of varying parameters may then be analyzed qualitatively using Cornu's spirals. We will use instead some representative graphs of the function $S_{\rm in}(k,\omega)$ as a basis for our discussion. The first few terms in the sum (3.15) are plotted separately in Figs. 8 and 9, where we have used the scaled frequency $\omega/\tilde{\omega}(T)$ in the abscissae. The effects of varying k are then clearly exhibited. In Fig. 8 we chose $k\tilde{l}=1$. The curves have single broad maxima, and the magnitude of the $n=2$ component is much smaller than that corresponding to $n=1$. In Fig. 9(a) we took $k\tilde{l}=5$. In agreement with the general predictions for class (b) potentials, additional oscillations appear in each component at frequencies *below* those corresponding to the main peak (cf. the results for the DP potential, where the oscillations begin to appear *above* the main peak). Finally, in Fig. 9(b) the value $k\tilde{l}=25$ was selected. A multiplicity of peaks is now present for all components. As in the case of the DP potential, a larger value of $k\tilde{l}$ results in an increase in the relative contributions of the higher-n terms. In addition, the high-frequency wing of each component is extended by increasing the magnitude of the transferred momentum. The dynamical structure factor has no quasielastic component: although $S_{\rm in}(k,\omega)$ is not strictly zero for any ω, it vanishes rapidly as $\omega\to 0$.

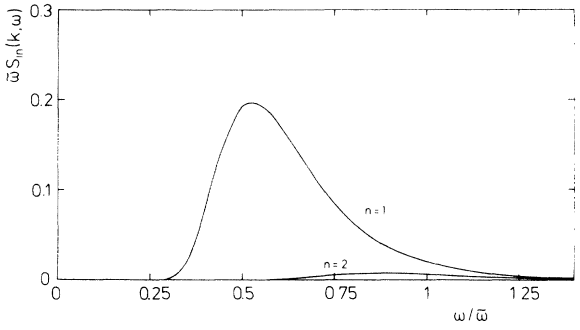

FIG. 8. Inelastic part of the DSF for the linear well potential as a function of the scaled frequency $\omega/\tilde{\omega}(T)$ for $k\tilde{l}=1$. The components are indicated next to the corresponding curves.

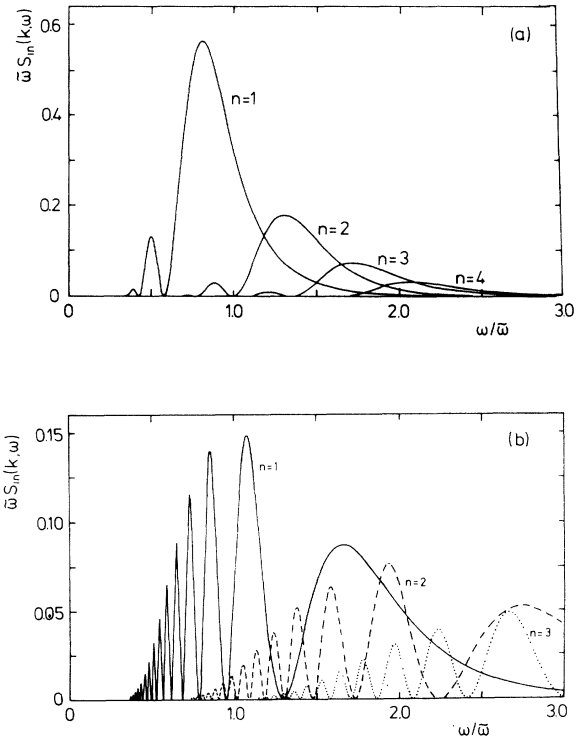

FIG. 9. Inelastic part of the DSF for the linear well potential as a function of the scaled frequency $\omega/\tilde{\omega}(T)$ for (a) $k\tilde{l}=5$ and (b) $k\tilde{l}=25$. The components are indicated next to the corresponding curves.

IV. IS THERE A QUASIELASTIC COMPONENT?

It is known that a quasielastic peak of the DSF results if the motion in a multiple-well potential is described by a Langevin equation with frictional and stochastic forces, or an equivalent Fokker-Planck equation.[30] We ask: Under which conditions is there a quasielastic component of $S(k,\omega)$ for one-dimensional Hamiltonian motion without such additional forces?

We can answer this question quite generally by deriving an upper bound to $S(k,\omega)$ and examining its behavior for small ω. Since the absolute value of the Fourier coefficients $F_{jn}(E,k)$ cannot be larger than one, an upper bound to $S(k,\omega)$ is obtained from expression (2.11) by replacing the square of the Fourier coefficients $|F_{jn}(E,k)|^2$ by one. In terms of a function $D(\omega)$, defined by

$$D(\omega)=Z^{-1}\sum_j \int_{E_{jl}}^{E_{ju}} dE\, e^{-\beta E} T_j(E)\delta[W_j(E)-\omega] , \quad (4.1)$$

we can write the inequality for $S(k,\omega)$, which defines the upper bound, as

$$S(k,\omega>0)\le \sum_{n=1}^{\infty}\frac{1}{n}D\left[\frac{\omega}{n}\right] . \quad (4.2)$$

Evaluating the energy integral in (4.1), we obtain

$$D(\omega)=\frac{2\pi}{\omega}Z^{-1}\sum_j [e^{-\beta E}|W_j'(E)|^{-1}]_{W_j(E)=\omega} , \quad (4.3)$$

where $W_j'(E)$ denotes the derivative of $W_j(E)$ with respect to E. If $W_j(E)=\omega$ holds for more than one energy in a given domain j, the different energies have to be summed over. We note in passing that, in the quantum-mechanical case, a similar upper bound exists, which represents the average density of final states for energy transfer $\hbar\omega$. If $D(\omega)$ goes to zero for $\omega\to 0$ faster than some positive power ω^{α} $(\alpha>0)$ of ω, the upper bound to $S(k,\omega)$ also tends to zero faster than ω^{α} for $\omega\to 0$. If this condition is valid, the dynamic structure factor has no quasielastic component.

For low ω only energy regions in which the oscillation frequency $W_j(E)$ is low contribute to $D(\omega)$. As follows from the results given in Sec. II A, these regions are (1) the uppermost energy region for potentials $V(x)$ which diverge like $|x|^q$ for $|x|\to\infty$ with $q<2$, (2) the vicinity of a minimum of the potential curve which is flatter than quadratic [i.e., $q>2$ in Eq. (2.3)], (3) the vicinity of a potential maximum which is either quadratic $(q=2)$ or flatter than quadratic $(q>2)$.

The contribution to $D(\omega)$ for small ω in either of the three cases is the following.

(1)

$$D(\omega)\sim\omega^{-4/(2-q)}\exp(-\text{const}/\omega^{2q/(2-q)}) \quad (\text{const}>0) .$$

(2)

$$D(\omega\sim\omega^{4/(q-2)} .$$

(3)

$$D(\omega)\sim\omega^{-3}\exp(-\text{const}/\omega) \quad (\text{const}>0)$$

in the case of a quadratic maximum. For a flatter maximum with $q>2$, the contribution to $D(\omega)$ is as in case (2).

In all three cases the condition given above for the absence of a quasielastic contribution to $S(k,\omega)$ is fulfilled. The condition can be violated only by choosing $q=\infty$ in cases (2) or (3). This corresponds to a potential with a completely flat bottom or barrier, like a square-well potential, a general single-well potential with a horizontal bottom, or a double-well potential with a horizontal barrier. In these cases the oscillation frequency $W(E)$ varies as $(E-E_0)^{1/2}$ for energies slightly above the energy E_0 of the horizontal portion of the potential curve. According to formula (1) this leads to a Gaussian shape proportional to $\exp(-C\omega^2)$ (with $C>0$) of the function $D(\omega)$ for small ω.

To illustrate how this Gaussian shape of $D(\omega)$ develops as the minimum or maximum of the potential curve becomes flatter and flatter, it is useful to consider a single-well power-law potential $V(x)=A|x|^q$ with arbitrary positive exponent q. The limiting case $q=\infty$ represents a square-well potential of width 2 with walls of infinite height. For this class of potentials the function $D(\omega)$ is readily calculated with the result given by

$$D(\omega)\propto\omega^{4/(q-2)}\exp(-C_q\omega^{2q/(q-2)}) , \quad (4.4)$$

where C_q is a positive q-dependent constant, which approaches a finite nonzero limit for $q\to\infty$. $D(\omega)$ has a single maximum, the position of which tends to zero proportionally to $q^{-1/2}$ for large q. For $q=\infty$, a Gaussian centered at the origin is obtained.

Coming back to the case of potential curves with a horizontal portion, we note that the upper bound (4.2) to $S(k,\omega)$ for small ω is a sum of Gaussians centered at the origin of ω. The expectation that $S(k,\omega)$ for small ω is also a sum of Gaussians is confirmed by the explicit calculation of $S(k,\omega)$ for a square-well potential given by

$$V(x)=\begin{cases}0 & \text{for } |x|<d/2 ,\\ \infty & \text{for } |x|>d/2 ,\end{cases}$$

which yields

$$S(k,\omega)=\frac{2(1-\cos kd)}{(kd)^2}\delta(\omega) + \left[\frac{8m\beta d^2}{\pi}\right]^{1/2}\sum_{n=1}^{\infty}(kd)^2\frac{[1-(-1)^n\cos kd]}{n[(kd)^2-(n\pi)^2]^2} \times\exp\left[-\frac{\beta m d^2\omega^2}{2\pi^2 n^2}\right] . \quad (4.5)$$

We have shown that, for regular potential functions $V(x)$, the dynamic structure factor does not contain a quasielastic component. A quasielastic component only exists if the potential curve has a strictly horizontal portion of finite width. Although potentials of this sort have been considered previously,[34,35] they appear somewhat artificial.

These results apply to strictly one-dimensional motion

without any coupling to additional degrees of freedom. As shown in the following section, such a coupling may generate a narrow quasielastic component of $S(k,\omega)$, the intensity of which is taken from the elastic line.

V. ELASTIC SCATTERING

The elastic component $S_{\rm el}(k,\omega)$ of the dynamic structure factor is given by the $n=0$ term of expression (2.11). Writing

$$S_{\rm el}(k,\omega)=S_0(k)\delta(\omega)\ , \tag{5.1}$$

we obtain for the elastic intensity

$$S_0(k)=Z^{-1}\sum_j\int_{E_{jl}}^{E_{ju}}dE\,e^{-\beta E}T_j(E)|F_{j0}(E,k)|^2 \tag{5.2}$$

with the $n=0$ Fourier coefficient given by

$$F_{j0}(E,k)=[T_j(E)]^{-1}\int_0^{T_j(E)}dt\,e^{ikx_j(E,t)}\ , \tag{5.3}$$

where again $x_j(E,t)$ is the solution of Newton's equation for energy E in domain j. $F_{j0}(E,k)$ is the average of $\exp(ikx)$, calculated with the sojourn probability density $p_{j,E}(x)$ in orbit (j,E):

$$p_{j,E}(x)=[T_j(E)]^{-1}\int_0^{T_j(E)}dt\,\delta[x_j(E,t)-x]$$
$$=[T_j(E)]^{-1}\{[E-V(x)]/(2m)\}^{-1/2}\ , \tag{5.4}$$

$$F_{j0}(E,k)=\int_{x_{j1}(E)}^{x_{j2}(E)}dx\,p_{j,E}(x)e^{ikx}$$
$$\equiv\langle e^{ikx}\rangle_{j,E}\ . \tag{5.5}$$

Recalling the second expression in (2.7) for the partition function Z, we may identify the elastic intensity given by (5.2) as the average of $|F_{j0}(E,k)|^2$ over all energies E and domains j. Denoting this average by a bar and using (5.5), we arrive at the formula

$$S_0(k)=\overline{|\langle e^{ikx}\rangle_{j,E}|^2}\ . \tag{5.6}$$

We remark that, with this notation, $\langle A\rangle=\overline{\langle A\rangle_{j,E}}$ for any function $A(x)$.

We wish to emphasize that for the derivation of this result (5.6) the strict periodicity of the Hamiltonian one-dimensional motion is essential. The periodicity of the orbital motion leads to infinitely long-lived correlations of the position coordinate x at different times, both for motion in single-well and multiple-well potentials. In the case of multiple-well potentials these correlations are, in part, due to the fact that, for energies below an energy barrier, the particle is trapped in the same well for all times. (The system is nonergodic.) The infinite persistence of correlations in time means that the system does not equilibrate. The result (5.6) only holds for nonequilibrating systems. For systems which equilibrate it has to be replaced by a different formula, which we are going to explain now.

To achieve equilibration, the one-dimensional motion needs to be coupled to other degrees of freedom, such as phonons. The coupling may be modeled by a Langevin equation, in which a frictional and a stochastic force are added to the conservative force deriving from the potential. In the equilibrating system the memory of the initial position $x(0)$ is lost after a sufficiently long time. Therefore, the correlation function (2.6), which, in our case of $f(x)=\exp(ikx)$ is called the intermediate scattering function, factorizes in the infinite-time limit:

$$\lim_{t\to\infty}\langle\exp\{ik[x(t)-x(0)]\}\rangle=|\langle e^{ikx}\rangle|^2\ . \tag{5.7}$$

We denote the rhs of this equation by $f(k)$. For the harmonic oscillator $f(k)$ is well known as the Debye-Waller factor, equal to $\exp(-k^2\langle x^2\rangle)$. We call $f(k)$ the Debye-Waller factor for a general anharmonic potential also. In the Fourier transform of the correlation function we find the infinite-time limit (5.7) as the coefficient of the δ function $\delta(\omega)$ which marks the elastic part. Therefore, the Debye-Waller factor $f(k)$ represents the intensity of the elastic component of $S(k,\omega)$ for an equilibrating system.

Comparing the elastic intensity $S_0(k)$ (5.6) and the Debye-Waller factor $f(k)$ (5.7) for a strictly one-dimensional Hamiltonian system, we note the inequality

$$S_0(k)\geq f(k)\ . \tag{5.8}$$

For an ideal harmonic oscillator this inequality has been known for a long time.[21,36–38] Let us assume that the coupling to additional degrees of freedom in an equilibrating system does not change the Debye-Waller factor f. This assumption is valid, eg., if the equilibrating system is described by a Langevin equation with a stochastic force of Gaussian white noise. The inequality (5.8) tells us that, in general, the elastic intensity is reduced in the equilibrating system. We wonder what happens with the missing elastic intensity given by the difference

$$S_0(k)-f(k)\ . \tag{5.9}$$

The example of the Brownian harmonic oscillator obeying a Langevin equation with a stochastic force of Gaussian white noise suggests the answer to this question. Because of the linearity of the Langevin equation for this system and the assumed Gaussian white noise of the stochastic force, the intermediate scattering function is easily calculated. The result reads

$$\langle\exp\{ik[x(t)-x(0)]\}\rangle$$
$$=\exp\{-k^2\langle x^2\rangle[1-\phi(t)]\} \tag{5.10}$$

with

$$\langle x^2\rangle=k_BT/(m\omega_0^2)$$

and

$$\phi(t)=\exp[-\zeta t/(2m)][\cos(\bar\omega t)+\zeta/(2m\bar\omega)\sin(\bar\omega t)]\ , \tag{5.11}$$

where ω_0 is the oscillator frequency, $\bar\omega=\{\omega_0^2-[\zeta/(2m)]^2\}^{1/2}$ and ζ the friction coefficient. The friction is assumed to be weak, i.e., $\zeta<2m\omega_0$. In the Taylor expansion of (5.10), the term of $0(k^4)$ contains a component proportional to $\exp(-\zeta t/m)$, which in the Fourier transform leads to a Lorentzian of half-width

ζ/m centered at $\omega=0$. For weak friction $\zeta \ll 2m\omega_0$, the intensity of this Lorentzian is just given by the difference (5.9), expanded to $0(k^4)$ (see below). It follows that, for weak friction, a part of the elastic line with an intensity given by (5.9) broadens into a narrow quasielastic component. We expect this result to be of general validity. Our argument is as follows. It is plausible to assume that the addition of a weak frictional and stochastic force appreciably changes the intermediate scattering function only for long times, as is the case in the example given by Eqs. (5.10) and (5.11). Therefore, the dynamic structure factor $S(k,\omega)$, which is the Fourier transform of the intermediate scattering function, should be affected only at low frequencies. If we assume further that the redistribution of spectral intensity over the frequency axis is continuous as frictional and stochastic forces are added, the effect must be a continuous broadening of the elastic line. We are thus led to the general conclusion that the essential modification of $S(k,\omega)$ by weak coupling to additional degrees of freedom, which enables the system to equilibrate, is the appearance of a narrow quasielastic component. The intensity of this component is subtracted from that of the elastic line. The limit of the quasielastic intensity for vanishing coupling strength is given by the difference (5.9). The usefulness of this result lies in the fact that (5.9) can be evaluated without solving a Langevin or Fokker-Planck equation.

We mention briefly that the above distinction between nonequilibrating and equilibrating system also plays a role in the calculation of the dynamic susceptibility $S(\omega)$ [Eq.(2.11) for $f(x)=x$] for one-dimensional motion in a double-well potential. For the Hamiltonian system, the nonergodicity of motion in a single well leads to an elastic component of intensity S_0 [cf. Eq. (5.1)]. Weak coupling to additional degrees of freedom, which makes the system ergodic, broadens the elastic line into a narrow quasielastic component. In the case of a Langevin equation with frictional and stochastic forces, the intensity of the quasielastic component in the limit of weak friction is equal to the intensity of the elastic component of the system without friction, which is readily calculated. It appears that this result has not been remarked upon in the previous treatments of the problem.[39–41]

The difference between the elastic intensity $S_0(k)$ and the Debye-Waller factor $f(k)$ for a one-dimensional Hamiltonian system is clarified by writing down the first terms of a cumulant expansion for each case. For the elastic intensity we obtain

$$S_0(k)=\exp[-\alpha(T)k^2+\delta(T)k^4+0(k^6)] \tag{5.12}$$

with

$$\alpha(T)=\overline{\langle(\Delta x)^2\rangle_{j,E}} \tag{5.13}$$

and

$$\delta(T)=\frac{\langle x^4\rangle}{12}-\frac{\overline{\langle x^3\rangle_{j,E}\langle x\rangle_{j,E}}}{3}+\frac{\overline{\langle x^2\rangle_{j,E}^2}}{4}-\frac{\alpha^2(T)}{2}\ , \tag{5.14}$$

or

$$\delta(T)=\tfrac{1}{4}\{\overline{\langle(\Delta x)^2\rangle_{j,E}^2}-[\overline{\langle(\Delta x)^2\rangle_{j,E}}]^2\}+\tfrac{1}{12}\{\overline{\langle(\Delta x)^4\rangle_{j,E}}-3[\overline{\langle(\Delta x)^2\rangle_{j,E}}]^2\}\ , \tag{5.15}$$

Here $\Delta x=x-\langle x\rangle_{j,E}$, where $\langle x\rangle_{j,E}$ is the average of the position coordinate in orbit (j,E). $\langle(\Delta x)^n\rangle_{j,E}$ is the average of $(\Delta x)^n$ in that orbit [cf., Eq.(5.5)]. As in Eq. (5.6), the bar denotes the canonical average over all orbits (j,E), e.g.,

$$\overline{\langle(\Delta x)^2\rangle_{j,E}}=Z^{-1}\sum_j\int_{E_{jl}}^{E_{ju}}dE\,e^{-\beta E}T_{j(E)}\langle(\Delta x)^2\rangle_{j,E}\ . \tag{5.16}$$

In (5.15) the first term on the rhs is positive definite; the second term may be positive or negative, but is probably small, since it vanishes in a Gaussian approximation. For the Debye-Waller factor one finds

$$f(k)=\exp[-\alpha'(T)k^2+\delta'(T)k^4+0(k^6)] \tag{5.17}$$

with

$$\alpha'(T)=\langle x^2\rangle-\langle x\rangle^2 \tag{5.18}$$

and

$$\delta'(T)=\frac{\langle x^4\rangle}{12}-\frac{\langle x^3\rangle\langle x\rangle}{3}+\frac{\langle x^2\rangle^2}{4}-\frac{[\alpha'(T)]^2}{2}\ . \tag{5.19}$$

A few important special cases are the following. For symmetric single-well potentials $\alpha=\alpha'$ since every orbit is symmetric around the origin (i.e., $\langle x\rangle_{j,E}=0$), but $\delta\neq\delta'$ because $\langle x^2\rangle^2\neq(\langle x^2\rangle_{j,E})^2$. For the harmonic oscillator δ' is zero, and δ is given by[21]

$$\delta(T)|_{\rm HO}=[k_BT/(2m\omega_0^2)]^2\ . \tag{5.20}$$

For symmetric double-well potentials with minima at $\pm l$ and frequency ω_0 for small-amplitude oscillations, we find, for temperatures low compared to the energy barrier,

$$\alpha(T)\approx k_BT/(m\omega_0^2)\ ,\qquad \alpha'(T)\approx l^2\gg\alpha(T)\ . \tag{5.21}$$

[For zero temperature $S_0(k)$ is unity trivially, and the Debye-Waller factor $f(k)$ oscillates as $\cos^2(kl)$, see below.]

The cumulant expansion is useful only for small values of k. Next we present exact results for the DP potential (3.1). The total intensity of the elastic line is conveniently written by separating the contributions of the lower and upper domains,

$$S_0(k)=S_0^<(k,T)+S_0^>(k,T)\ , \tag{5.22}$$

for which we obtain

$$S_0^<(k,T)=\frac{4\pi Q}{\omega_0 Z}\int_0^1 dx\,e^{-\beta Qx}|J_0(kl x^{1/2})|^2 \tag{5.23}$$

and

$$S_0^{>}(k,T)=\frac{2Q}{\pi\omega_0 Z}\int_1^{\infty}dx\, e^{-\beta Q x}\rho(x)|h(x)|^2 , \quad (5.24)$$

with $x=E/Q$, $\rho(x)=1+(2/\pi)\Psi(x)$, and

$$h(x)=\int_0^{\pi}dy\,\cos(kl\{1+x^{1/2}\sin[\rho(x)y-\Psi(x)]\}) . \quad (5.25)$$

The coefficient α of the leading term in the cumulant expansion (5.12) is given by

$$\alpha(T)=\frac{2\pi l^2}{\omega_0\beta Z}\left\{\frac{1}{2\beta Q}[2-(1-\beta Q)e^{-\beta Q}]+\frac{4}{\pi(\beta Q)^{1/2}}\Gamma(3/2,\beta Q)\right\} , \quad (5.26)$$

where $\Gamma(3/2,\beta Q)$ is the incomplete γ function. The Debye-Waller factor, on the other hand, is given by

$$f(k,T)=\left[\frac{2\pi Q}{\omega_0 Z}\right]^2\left|2\cos(kl)\int_0^1 dx\, e^{-\beta Q x}J_0(klx^{1/2})+\frac{1}{\pi}\int_1^{\infty}dx\,\rho(x)e^{-\beta Q x}h(x)\right|^2 . \quad (5.27)$$

In Fig. 10, we show the amplitude of the elastic line as a function of the temperature for two values of kl. At low temperatures only the vicinity of the potential minima contributes, and only the k^2 term in the cumulant expansion is significant. In agreement with Eqs. (5.12) and (5.21), $\ln[S_0(k)]\simeq -k^2\langle(\Delta x)^2\rangle$, with $\langle(\Delta x)^2\rangle\simeq k_BT/m\omega_0^2$. At higher temperatures we find strong deviations from this simple behavior. For small values of the momentum transfer ($kl\lesssim 1$), the magnitude of the elastic line decreases faster than would be expected from Eq. (5.21), while for higher values of kl the decrease is slower than expected. However, if $k_BT/Q\gg 1$ (a region not shown in Fig. 10), the contributions come mainly from the upper domain and we regain the high-T simple harmonic oscillator form $S_0(k,T)\sim(\pi k_BT)^{-1/2}(kl)^{-1}$.

In Fig. 11, we plot $S_0(k,T)$ and the Debye-Waller factor $f(k,T)$ for a low value of k, so both functions are well described by the k^2 term in the cumulant expansion. The asymptotic low-temperature forms are indicated by the dashed lines. The strong deviation of the elastic intensity from a linear T dependence is observed again. The variation of $f(k,T)$ is much smoother, and both functions converge at high temperatures.

A detailed comparison of $S_0(k,T)$ and $f(k,T)$ is presented in Fig. 12, where they are plotted as functions of the momentum transfer for three values of the temperature. Let us first consider the magnitude S_0 of the elastic line in the absence of friction. This is a monotonically decreasing, but somewhat bumpy, function of kl. The bumps are due to the contribution of the upper domain, which shows wide maxima and minima. However, the decay of the contribution of the lower domains is so strong that this structure only appears as a perturbation in the slope of the total function. For a fixed value of kl, $S_0(k,T)$ is also a monotonically decreasing function of T. This was to be expected from the discussion above, since the nonergodic contribution must become smaller at high temperatures.

As mentioned above, at $T=0$, $S_0(k)$ is unity, and the Debye-Waller factor $f(k)$ oscillates as $\cos^2(kl)$. The maxima of $f(k)$ occur when the transformed wavelength fits an integer number of times in the distance $2l$ between wells. Under "antiresonance" conditions [$kl=(2n+1)\pi/2$, n integer], the Debye-Waller factor

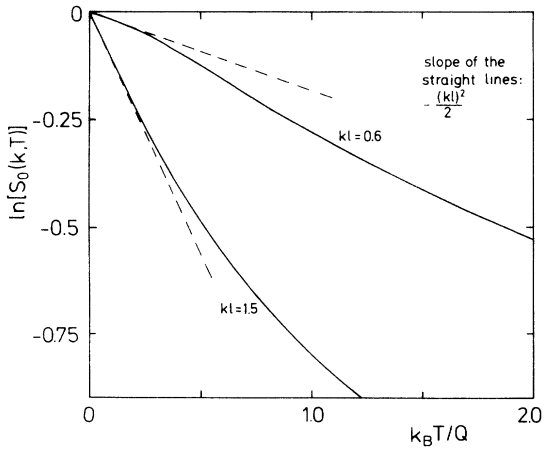

FIG. 10. Intensity of the elastic line as a function of temperature for the DP potential at the indicated values of kl. The dashed lines represent the leading term [up to $O(k^2)$] in the cumulant expansion.

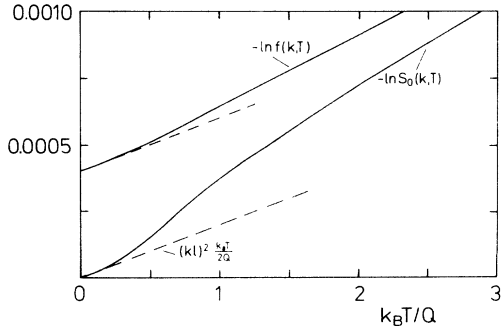

FIG. 11. DP potential: minus the logarithms of the elastic intensity and the DW factor as functions of the temperature for $kl=0.02$. The cumulant expansion truncated to order k^2 is valid over the whole range considered.

disappears completely. As shown above, if weak friction and stochastic forces are added to our Hamiltonian model, the elastic intensity is reduced to the Debye-Waller factor $f(k)$, and the difference $S_0(k)-f(k)$ yields the intensity of a narrow quasielastic line. With the zero-temperature results for $S(k)$ and $f(k)$ just stated, these intensities are identical with those obtained for a jump model with jumps occurring between two equivalent sites separated by the distance $2l$.[25] For the jump model the quasielastic line is a Lorentzian with a half-width given by twice the jump rate.

At nonzero, but low, temperatures, only the lower domains of the DP wells contribute and the zeros and maxima shift toward lower values of the momentum transfer. This can be seen by writing $y=klx^{1/2}$ in the first term on the right-hand side of Eq. (5.27): then it becomes obvious that the temperature appears only through the combination $\beta Q/(kl)^2$. The Debye-Waller factor shows a peculiar behavior as a function of the temperature if we fix kl. Although it decreases with increasing temperature for small values of k, it can have strong oscillations as a function of T in the region near $kl=\pi/2$. This can also be seen from Fig. 12, where, for $kl\approx 1.6$, the result for $k_BT/Q=0.1$ is between those for $k_BT/Q=1$ and 10. Again, the distance between the curves for $S_0(k,T)$ and $f(k,T)$ gives the intensity of the quasielastic component in the case of a finite, but very small, friction. This difference is very large near $kl=(2n+1)\pi/2$ at low temperatures.

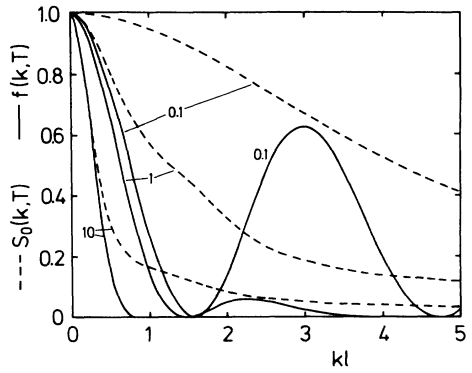

FIG. 12. Intensity of the elastic line (dashed) and DW factor (solid line) as functions of the momentum transfer for the DP potential at the indicated values of k_BT/Q.

Finally, we give the magnitude of the elastic line for the linear single-well potential:

$$S_0(k)=\frac{2}{\pi^{1/2}}\int_0^\infty d\xi\,\xi^{1/2}e^{-\xi}\left|\int_0^1 dx\,\cos[k\bar{l}(T)\xi(x^2-x)]\right|^2 . \tag{5.28}$$

If $k\bar{l}(T)\to 0$,

$$S_0(k)\sim\exp[-k^2\bar{l}^2(T)/8] . \tag{5.29}$$

Note that, in this case, $\langle x^2\rangle=\bar{l}^2(T)/8=2(k_BT/\alpha)^2$.

VI. DIRECTIONAL AND CONFIGURATIONAL AVERAGES

In the previous sections we considered ensembles of particles moving in identical one-dimensional potentials oriented in the same spatial direction. It is useful to analyze separately two possible generalizations of the problem and to indicate what may be expected from them.

A. Directional average

Consider a three-dimensional sample containing a distribution of one-dimensional, identical, but randomly oriented scattering centers. This could be the case, for instance, with the double-well structures in glasses. Since in an experiment the direction of $\mathbf{k}$ is specified by the position of the detector, we must perform an angular average over the contributions of the randomly oriented scatterers. If the unit vector $\hat{l}$ defines the orientation of a scatterer, i.e., the direction of its one-dimensional motion, it is easy to see that the directional average of a function $g(\mathbf{k}\cdot\hat{l})$ may be evaluated as

$$\langle g(\mathbf{k}\cdot\hat{l})\rangle_{\rm dir}=\frac{1}{2k}\int_{-k}^{k}d\eta\,g(\eta) . \tag{6.1}$$

In the evaluation of $S(\mathbf{k},\omega)$, the angle between $\mathbf{k}$ and $\hat{l}$ appears only in the Fourier coefficients, so we can carry out the directional average $\langle|F_{jn}(E,\mathbf{k}\cdot\hat{l})|^2\rangle_{\rm dir}$ for each value of the energy. From Eq. (6.1) we see that, for a given $\mathbf{k}$, all values of the momentum transfer having a magnitude smaller than k contribute to the signal. This admixture of momentum transfer values introduces two important modifications into our description of $S(k,\omega)$. First, it destroys the intraband peak structure in the inelastic region. The band structure itself, being independent of the momentum transfer, is preserved. Second, the intensity of the upper bands, which grows when the magnitude of the momentum transfer is increased, decreases in favor of the elastic line and the lowest band.

These modifications are clearly exhibited by the results of the directional average of the DP results. For the contribution of the lower domains, we see from Eqs. (3.6) and (6.1) that the intensity of the elastic line is increased because the average of $|J_0(x)|^2$ over the values from $x=0$ to $x_{\max}$ is always larger than $|J_0(x_{\max})|^2$, at least for $x_{\max}\le j_{00}$, the first zero of $J_0(x)$. The opposite is true for the other peaks because the higher-order Bessel functions are increasing functions of x, at least for small and moderate values of x.

A similar effect occurs with the contributions of the upper domain. By making the effective k smaller, the directional average transfers intensity from the upper bands in $S_{\rm in}$ to the lowest one. Due to the admixture of values of the effective momentum transfer, the minima

inside each band disappear and the center of gravity of each band is shifted to higher frequencies. This is seen in Fig. 4, where the directional average is indicated by a dashed line. By expanding the cosine in the integral in Eq. (5.25), it is also easy to verify that, at least for kl small enough, the contribution of the upper domain to the elastic line is increased by the directional average.

We note that the directional average of $S(k,\omega)$ has been used, in the tunneling limit, to interpret data for H tunneling in niobium.[23,42] Buchenau *et al.* also obtained the averaged coherent neutron cross section, considering that the particle can jump between two fixed positions in a double well.[6]

B. Configurational average

We know how to evaluate $S(k,\omega)$ for a particular set of parameters $\{\alpha_j\}$ characterizing the one-dimensional potential under consideration. It is, in principle, possible to make a sample containing a distribution of identical defects (say, by a clever addition of impurities). However, in a system like a glass or a protein we expect to find a distribution of potential parameters (barrier height, asymmetry, etc.) characterizing the potential wells.[2,3,7,43,44] To compare the theoretical predictions with experimental results, we must perform a suitable average over the parameters. Suppose that the parameter distribution is given by the function $P\{\alpha_j\}$. We must then calculate an average over potential configurations,

$$\langle S(k,\omega)\rangle_{\text{conf}}=\frac{\int d\{\alpha_j\}S(k,\omega;\{\alpha_j\})P(\{\alpha_j\})}{\int d\{\alpha_j\}P(\{\alpha_j\})} . \quad (6.2)$$

It is obvious that the survival of the peak structure will depend on the width of the parameter distribution. As an example, we select again the DP potential. For this potential two parameters are available, ω_0 and l, or, alternatively, Q and l. The respective distributions are related by $m\omega_0 l^2 P_1(Q,l)=P_2(\omega,l)$. A simplified possibility is to assume that the individual wells have all the same shape, i.e., the same ω_0, but that the interwell distance l is a random variable with a Gaussian distribution of width L around an average value l_0,

$$P(l)\sim\exp[-(l_0/L)^2(1-l/l_0)^2] .$$

In Fig. 13, we have plotted the average of $S(10,\omega)$ at $k_BT/Q=10$ using this distribution for the values $l_0/L=30$ and 10. In this case the thin-peak structure is very sensitive to the averaging. For $l_0/L=30$, the upper peaks have already been completely smeared out; the height of the remaining maxima has decreased (cf., Fig. 6) and the minima have nonzero magnitudes. For $l_0/L=10$, the peak structure has disappeared completely. For smaller values of l_0/L (not shown in the figure), the position of the maximum shifts slightly to higher frequencies and its magnitude decreases. A high-frequency tail appears due to those potentials in the distribution for which l is very small and where, at the temperature considered, the particle oscillates with a frequency very close to ω_0.

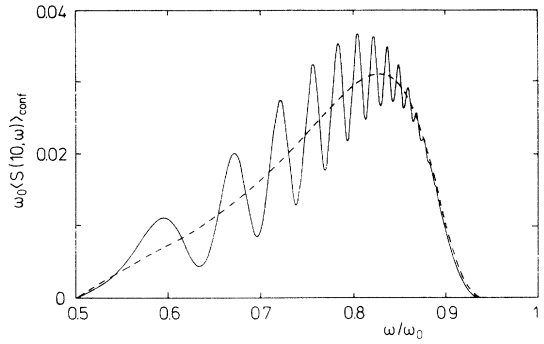

FIG. 13. Configurational average of $S_{in}(k,\omega)$ for the first band of the DP potentials. Gaussian distributions of interwell distances were chosen with inverse widths $l_0/L=30$ (solid line) and $l_0/L=10$ (dashed line). Here $k_BT/Q=10$ and $kl=10$.

VII. CONCLUSION

We have performed a detailed analysis of the dynamic structure factor associated with classical Hamiltonian motion in one-dimensional, single- and multiple-well potentials. Our main results can be summarized as follows.

(a) The relation between the intensity of the elastic line and the Debye-Waller factor was clarified. The Debye-Waller factor gives the surviving elastic intensity when a small amount of friction is added and the long-time correlations due to periodic motion are destroyed. We argue that the difference between the magnitude of the elastic line for the Hamiltonian problem and the Debye-Waller factor appears as a quasielastic component when weak frictional forces are present.

(b) The dynamical structure factor cannot contain a quasielastic component unless there is a region where the potential is a constant. In this case, $S(k,\omega)$ contains a superposition of Gaussians centered at $\omega=0$. Otherwise, quasielastic peaks can only occur in the presence of frictional forces.

(c) The structure of $S(k,\omega)$ in the elastic region is closely related to the asymptotic form of the potential. When the potential does not diverge faster than x^2 as $x\to\infty$, and when the values of the temperature and the momentum transfer are high enough, a plot of $S(k,\omega)$ as a function of ω may exhibit a large number of peaks. For potentials that diverge as x^2 when $x\to\infty$, the peaks emerge near the upper end of the contribution of each Fourier component, i.e., "band." If the potential diverges more slowly than x^2 as $x\to\infty$, the oscillations appear at the lower end of each band. The effects of varying the temperature and the transferred energy and momentum were illustrated with two specific examples. We have not taken into account the effect of fluctuating forces such as due to phonons, which could be modeled by random forces and an effective friction. We may expect the peak structure of the inelastic region of $S(k,\omega)$ to be smeared by the introduction of a small amount of friction. A detailed investigation of this effect remains an open interesting question.

(d) The effects of directional and configurational averages were investigated. In the first case the average is carried out over spatial orientations, while in the second it is performed over a distribution of parameters characterizing the potentials. Both procedures lead to a smearing out of the oscillations inside each Fourier component. The directional average also results in an intensity transfer from the upper to the lower bands.

ACKNOWLEDGMENTS

Financial assistance by the German Bundesministerium für Forschung und Technologie (Project No. 03-JA2KON-1) and by the Deutsche Forschungsgemeinschaft through the Sonderforschungsbereich 306 is gratefully acknowledged. This research was also supported by an award from the Research Corporation.

[1]P. W. Anderson, B. I. Halperin, and C. M. Varma, Philos. Mag. **25**, 1 (1972).
[2]W. A. Phillips, J. Low Temp. Phys. **7**, 351 (1972).
[3]W. A. Phillips, Rep. Prog. Phys. **50**, 1657 (1987).
[4]H. R. Schober and U. Buchenau, in *Phonons 89*, edited by S. Hunklinger, W. Ludwig, and G. Weiss (World Scientific, Singapore, 1990), Vol. 1.
[5]M. I. Klinger, Phys. Rep. **165**, 275 (1988).
[6]U. Buchenau, H. M. Zhou, N. Nucker, K. S. Gilroy, and W. A. Phillips, Phys. Rev. Lett. **60**, 1318 (1988).
[7]Yu. M. Galperin, V. G. Karpov, and V. I. Kozub, Adv. Phys. **38**, 669 (1989).
[8]M. I. Klinger, Phys. Lett. A **144**, 97 (1990).
[9]U. Buchenau, Yu. M. Galperin, V. L. Gurevich, and H. R. Schober, Phys. Rev. B **43**, 5039 (1991).
[10]J. Smith *et al.*, J. Chem. Phys. **85**, 3636 (1986).
[11]W. Doster, S. Cusack, and W. Petry, Nature **337**, 754 (1989).
[12]J. Smith, K. Kuczera, and M. Karplus, Proc. Natl. Acad. Sci. USA **87**, 1601 (1990).
[13]P. Martel, P. Calmettes, and B. Hennion, Biophys. J. **59**, 363 (1991).
[14]J. Zollfrank, J. Friedrich, J. M. Vanderkooi, and J. Fidy, Biophys. J. **59**, 305 (1991).
[15]C. A. Condat and J. Jäckle, J. Phys. A **24**, 985 (1991).
[16]M. E. Lines and A. M. Glass, *Principles and Applications of Ferroelectrics and Related Materials* (Clarendon, Oxford, 1977).
[17]V. L. Aksenov, N. M. Plakida, and S. Stamenkovic, *Neutron Scattering by Ferroelectrics* (World Scientific, Singapore, 1990).
[18]Y. Onodera, Prog. Theor. Phys. **44**, 1477 (1970).
[19]T. Matsubara, Prog. Theor. Phys. **48**, 351 (1972).
[20]M. Iwamatsu and Y. Onodera, Prog. Theor. Phys. **57**, 699 (1977).
[21]C. M. Vineyard, Phys. Rev. **110**, 999 (1959).
[22]Y. Imry, in *Tunneling Phenomena in Solids*, edited by E. Burstein and S. Lundquist (Plenum, New York, 1969).
[23]H. Wipf, A. Magerl, S. M. Shapiro, S. K. Satija, and W. Thomlinson, Phys. Rev. Lett. **46**, 947 (1981).
[24]T. Springer, *Quasielastic Neutron Scattering for the Investigation of Diffusive Motions in Solids and Liquids*, Springer Tracts in Modern Physics (Springer, Berlin, 1972).
[25]M. Bée, *Quasielastic Neutron Scattering* (Hilger, Bristol, 1988).
[26]D. Richter and T. Springer, Phys. Rev. B **18**, 126 (1978).
[27]J. W. Haus and K. W. Kehr, Phys. Rep. **150**, 263 (1987).
[28]K. Funke, Z. Phys. Chem. Neue Folge **154**, 251 (1987).
[29]R. Schilling and S. Aubry, J. Phys. C **20**, 4881 (1987).
[30]W. Dieterich, T. Geisel, and I. Peschel, Z. Phys. B **29**, 5 (1978).
[31]See, for example, F. Yoshida and S. Takeno, Phys. Rep. **173**, 301 (1989).
[32]See, for example, J. Mayers, Phys. Rev. B **41**, 41 (1990), and references therein.
[33]C. Benoit, J. Phys. Condens. Matter **1**, 335 (1989).
[34]J. G. Kincaid and H. Eyring, J. Chem. Phys. **5**, 587 (1937).
[35]J. G. Dash, D. P. Johnson, and W. M. Visscher, Phys. Rev. **168**, 1087 (1968).
[36]H. Ott, Ann. Phys. (Leipzig) **23**, 169 (1935).
[37]B. Kaufman and H. Lipkin, Ann. Phys. (N.Y.) **18**, 294 (1962).
[38]A. A. Maradudin, Rev. Mod. Phys. **36**, 417 (1964).
[39]K. Voigtländer and H. Risken, J. Stat. Phys. **40**, 397 (1985).
[40]M. I. Dykman, S. M. Soskin, and M. A. Krivoglaz, Physica A **133**, 53 (1985).
[41]M. I. Dykman *et al.*, Phys. Rev. A **37**, 1303 (1988).
[42]K. Neumaier, D. Steinbinder, H. Wipf, H. Blank, and G. Kearley, Z. Phys. B **76**, 359 (1989).
[43]W. Köhler and J. Friedrich, Phys. Rev. Lett. **59**, 2199 (1987).
[44]R. Hirschmann, J. Friedrich, and E. Daltrozzo, J. Chem. Phys. **91**, 7296 (1989).